PERSPECTIVE OPEN

Check for updates

# Trompe L'oeil Ferromagnetism—magnetic point group analysis

Sang-Wook Cheong[1]✉ and Fei-Ting Huang[1]

Ferromagnetism can be characterized by various distinct phenomena such as non-zero magnetization (inducing magnetic attraction/repulsion), diagonal piezomagnetism, nonreciprocal circular dichroism (such as Faraday effect), odd-order (including linear) anomalous Hall effect, and magneto-optical Kerr effect. We identify all broken symmetries requiring each of the above phenomena, and also the relevant magnetic point groups (MPGs) with those broken symmetries. All ferromagnetic point groups, relevant for ferromagnets, ferrimagnets, and weak ferromagnets, can certainly exhibit all these phenomena, including non-zero magnetization. Some of the true antiferromagnets, which are defined as magnets with MPGs that do not belong to ferromagnetic point groups, can display these phenomena through magnetization induced by external perturbations such as applied current, light illumination, and uniaxial stress, which preserve the combined symmetry of spatial inversion together with time reversal. Such MPGs are identified for each external perturbation. Since high-density and ultrafast spintronic technologies can be enabled by antiferromagnets, our findings will be essential guidance for future magnetism-related science as well as technology.

*npj Quantum Materials* (2023)8:73 ; https://doi.org/10.1038/s41535-023-00603-5

## INTRODUCTION

Magnetic states exhibiting non-zero net magnetization include ferromagnets, ferrimagnets, or weak ferromagnets (including canted antiferromagnets). Due to the non-zero magnetization, those magnetic states exhibit physical phenomena[1–13] such as magnetic attraction, various magneto-optical properties (magneto-optical Kerr (MOKE), Faraday, and magnetic circular dichroism), and anomalous Hall-type effects. The anomalous Hall-type effects manifest anomalous Hall, anomalous Ettingshausen, anomalous Nernst, or anomalous thermal Hall effects[7,12,14–18]. It turns out that these phenomena that usually occur only in magnetic states with non-zero magnetization can take place in certain antiferromagnets with seemingly zero net magnetization[14,17,19–21], sometimes in the presence of external perturbations such as stress, electric current, or light ilumination. These cases have been called Trompe L'oeil Ferromagnetism[22].

It turns out that broken symmetries can be associated with order parameters and emergent phenomena. Herein, we meticulously outline the precise broken symmetries associated with each of these phenomena: non-zero magnetization, diagonal piezomagnetism[2,23], circular dichroism[24–26], nonreciprocal circular dichroism (such as Faraday effect)[27], odd-order (including linear) anomalous Hall effect (AHE), and MOKE[13,28]. Notably, the constraints imposed by symmetry on equilibrium-property tensors, combined with an in-depth MPGs analysis, have been established. For a more comprehensive understanding, readers are encouraged to the provided references[1–3,23,29–31]. In this perspective, instead, we utilize the concept of Symmetry Operational Similarity (SOS)[29] for these analyses and classify the corresponding magnetic point groups (MPGs) with those broken symmetries, i.e., each of the above phenomena.

Observable physical phenomena can occur or non-zero measurable can be detected when specimens have SOS with the combination of measurable (or experimental setup for measurable) and specimen environments (such as applied external stress, electric fields, or magnetic fields), or specimens with specimen environments have SOS with measurable. This SOS relationship includes when specimens have more, but not less, broken symmetries than the combination of measurable and specimen environments or specimens with specimen environments have more, but not less, broken symmetries than measurable. In other words, to have a SOS relationship, specimens cannot have higher symmetries than the combination of measurable and specimen environments or specimens with specimen environments cannot have higher symmetries than measurable. Our SOS approach, considering the group symmetry of the whole experimental setup, is in accordance with the well-known Neumann's Principle[1,32], and its power lies in providing simple and physically transparent views of otherwise unintuitive phenomena in complex materials, without considering specific coupling terms or the relevant Hamiltonians. Furthermore, this approach has the capability to connect seemingly unrelated phenomena in systematic ways and can be employed to discover potential materials with potentially desirable properties, as well as uncover exciting phenomena in existing materials.

To find the requirements of broken symmetries for various phenomena, we, first, define the general symmetry operation notations for three orthogonal *x*, *y*, and *z* axes such as $\mathbf{R_x}$ = 2-fold rotation around the *x*-axis, $\mathbf{M_x}$ = mirror reflection with mirror perpendicular to the *x* axis, $\mathbf{I}$ = space inversion, $\mathbf{T}$ = time reversal, etc. Then, we have these general relationships: $\mathbf{R_x}\otimes\mathbf{R_y} = \mathbf{R_z}$, $\mathbf{M_z}\otimes\mathbf{R_y} = \mathbf{M_x}$, $\mathbf{M_x}\otimes\mathbf{R_z} = \mathbf{M_y}$, $\mathbf{M_x}\otimes\mathbf{R_y} = \mathbf{M_z}$, $\mathbf{M_y}\otimes\mathbf{M_z} = \mathbf{R_x}$, $\mathbf{M_x}\otimes\mathbf{M_z} = \mathbf{R_y}$, $\mathbf{M_x}\otimes\mathbf{M_y} = \mathbf{R_z}$, $\mathbf{M_x}\otimes\mathbf{R_x} = \mathbf{M_y}\otimes\mathbf{R_y} = \mathbf{M_z}\otimes\mathbf{R_z} = \mathbf{I}$, $\mathbf{M_x} = \mathbf{R_x}\otimes\mathbf{I}$, $\mathbf{M_y} = \mathbf{I}\otimes\mathbf{R_y}$, and $\mathbf{M_z} = \mathbf{I}\otimes\mathbf{R_z}$. All are commutative operations. Measurables such as magnetization or optical activity setups have translational symmetry, so we can ignore or freely allow any translations, i.e., any translations are considered as a unit operation. Similarly, when we consider one-dimensional (1D) measurables invariant under any rotations along the 1D direction, then we ignore or freely allow any rotations around the axis, i.e., any rotations around the 1D direction are considered as a unit operation. For example, magnetization along *z* should be invariant

[1]Rutgers Center for Emergent Materials and Department of Physics and Astronomy, Rutgers University, Piscataway, NJ 08854, USA. ✉email: sangc@physics.rutgers.edu

under any rotations along $z$, so we ignore or freely allow any rotations around $z$[33,34].

## SYMMETRY OF FERROMAGNETISM

Magnetization ($\boldsymbol{M}$) along $z$, which is a 1D object along $z$, has broken $\{\mathbf{I}\otimes\mathbf{T},\mathbf{T},\mathbf{M_x},\mathbf{M_y},\mathbf{R_x},\mathbf{R_y},\mathbf{C_{3x}},\mathbf{C_{3y}}\}$ and unbroken $[\mathbf{1},\mathbf{I},\mathbf{M_z},\mathbf{R_z}]$, and thus has broken $\{\mathbf{I}\otimes\mathbf{T},\mathbf{T},\mathbf{M_x},\mathbf{M_y},\mathbf{R_x},\mathbf{R_y},\mathbf{C_{3x}},\mathbf{C_{3y}}\}$ with free rotation along $z$. As discussed above, when we consider the symmetry of 1D objects such as $\boldsymbol{M}$, we always allow any free rotations along the 1D direction. For example, $\bar{4}'$ has unbroken $\mathbf{C_{4z}}\otimes\mathbf{I}\otimes\mathbf{T}$ and broken $\mathbf{I}\otimes\mathbf{T}$, but when we consider the SOS relationship of $\bar{4}'$ with a 1D object along $z$, then $\bar{4}'$ has unbroken $\mathbf{I}\otimes\mathbf{T}$ with free rotation along $z$, so $\bar{4}'$ does not have SOS with $\boldsymbol{M_z}$. All and also only MPGs, belonging to the ferromagnetic point groups, do have broken $\{\mathbf{I}\otimes\mathbf{T},\mathbf{T},\mathbf{M_x},\mathbf{M_y},\mathbf{R_x},\mathbf{R_y},\mathbf{C_{3x}},\mathbf{C_{3y}}\}$ with free rotation along $z$ or the relevant requirements along $x$ or $y$. The thirty-one (31) ferromagnetic point groups include 1, $\bar{1}$, 2, 2′, $m$, $m'$, 2/$m$, 2′/$m'$, 2′2′2, $m'm'm$, $m'm'2$, $m'm2'$, 4, $\bar{4}$, 4/$m$, 42′2′, 4$m'm'$, $\bar{4}$2′$m'$, 4/$mm'm'$, 3, $\bar{3}$, 32′, 3$m'$, $\bar{3}m'$, 6, $\bar{6}$, 6/$m$, 62′2′, 6$m'm'$, $\bar{6}m'$2′, 6/$mm'm'$[2,31]. Note that $\bar{4}'$ does not belong to the ferromagnetic point groups.

The presence of non-zero net magnetization in magnetic states in ferromagnetic point groups is sometimes evident, but it is not always. For example, magnetic states depicted in Fig. 1a–d appear to be antiferromagnetic states with 120° spins without any net magnetic moments. However, all belong to ferromagnetic point groups; Fig. 1a; $mm'm'$, which has been observed in $Mn_3Sn$ ($Cmc'm'$)[9], Fig. 1b; $m'mm'$, which has been observed in $Mn_3$(Ge,Ga) ($Cm'cm'$), Fig. 1c; 2/$m$; kagome lattice with lattice distortions, shown with solid-line bonds ($P2_1/n$)[35], and Fig. 1d; $\bar{3}m'$, which has been observed in $Mn_3$(Rh,Ir,Pt) ($R\bar{3}m'$)[7,36]. Kagome layer in Fig. 1(d) corresponds to the MPG 6′/$m'm'm$, which does not belong to the ferromagnetic point group; however, ABC-type stacking of kagome layers results in the MPG $\bar{3}m'$, which now belongs to the ferromagnetic point group. Indeed, small but non-zero magnetization has been observed, at least, in $Mn_3Sn$ and $Mn_3$(Ge,Ga)[15,28].

## SYMMETRY OF THE ODD-ORDER AHE MEASUREMENTS

The Hall effect was discovered by Edwin Hall while he was working on his doctoral degree in 1879, and has been well utilized to measure carrier density as well as detect small magnetic fields[37]. This so-called ordinary Hall effect contrasts with the anomalous Hall effect (AHE) in ferromagnets, which is sometimes called extraordinary Hall effect or spontaneous Hall effect[18]. This AHE exists in zero applied magnetic field, and varies linearly with applied electric current, so its sign changes when the current direction is reversed. It was proposed that AHE can exist in truly antiferromagnetic systems such as $Mn_3$(Rh,Ir,Pt) with Kagome lattice[7,36], originating from the Berry curvature. In fact, $Mn_3$(Sn,Ge), forming in the same crystallographic structure as that of $Mn_3$(Rh,Ir,Pt), is experimentally reported to exhibit a significant AHE[9,14]. However, it turns out that $Mn_3$(Sn,Ge) does exhibit a small, but finite net magnetic moment[15,28], and the exact experimental situation of $Mn_3$(Rh,Ir,Pt) is presently unclear, partially due to the presence of competing multiple magnetic states in the system, and also the absence of bulk crystal study. Topological Hall effects in skyrmion systems have been reported[38,39], and occur typically in the presence of external magnetic fields. Note that AHE of antiferromagnets with zero or small magnetization can be particularly useful for the fast sensing of magnetic fields due to the intrinsic fast dynamics of antiferromagnets[40].

Herein, we define AHE as transverse voltage induced by applied current in zero magnetic fields. The sets of (electric current, $+/-$), (electric current, h/c), (thermal current, $+/-$), and (thermal current, h/c) correspond to the Hall, Ettingshausen, Nernst, and thermal Hall effects, all of which we call Hall-type effects, respectively (+/-

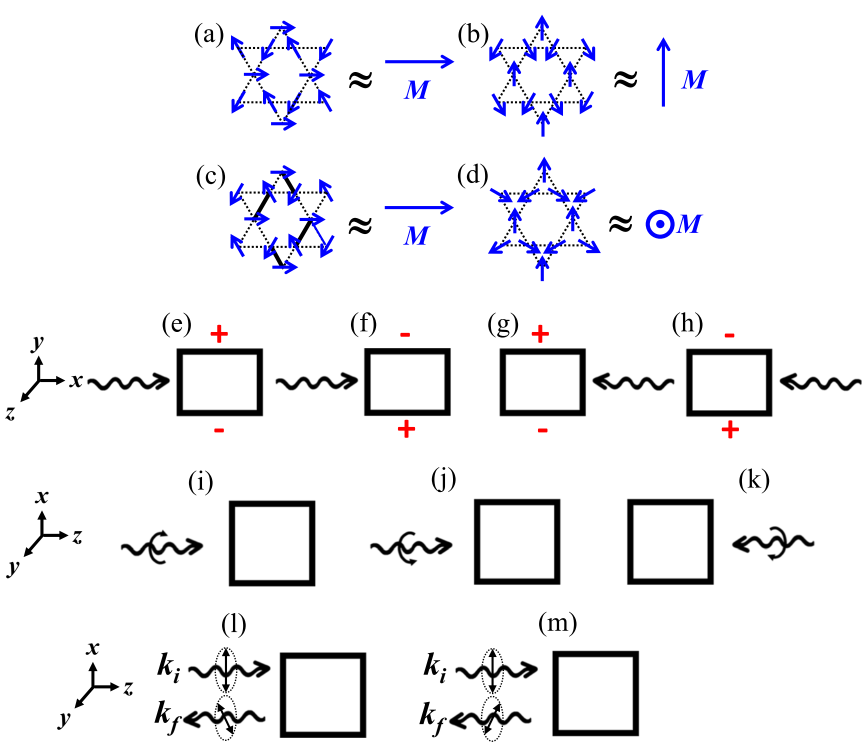


**Fig. 1 Various specimens and experimental setups for AHE, circular dichroism and MOKE. a**–**d** are for $Mn_3Sn$ ($Cmc'm'$), $Mn_3$(Ge,Ga) ($Cm'cm'$), kagome lattice with lattice distortions, shown with solid-line bonds ($P2_1/n$), and one (6′/$m'm'm$) of three stacked kagome layers in $Mn_3$(Rh,Ir,Pt) ($R\bar{3}m'$), respectively. **e**–**h** Four experimental setups to measure AHE, i.e., transverse voltage induced by current. **i**–**k** Three experimental setups to measure circular dichroism. **l**, **m** Two experimental setups to measure MOKE.

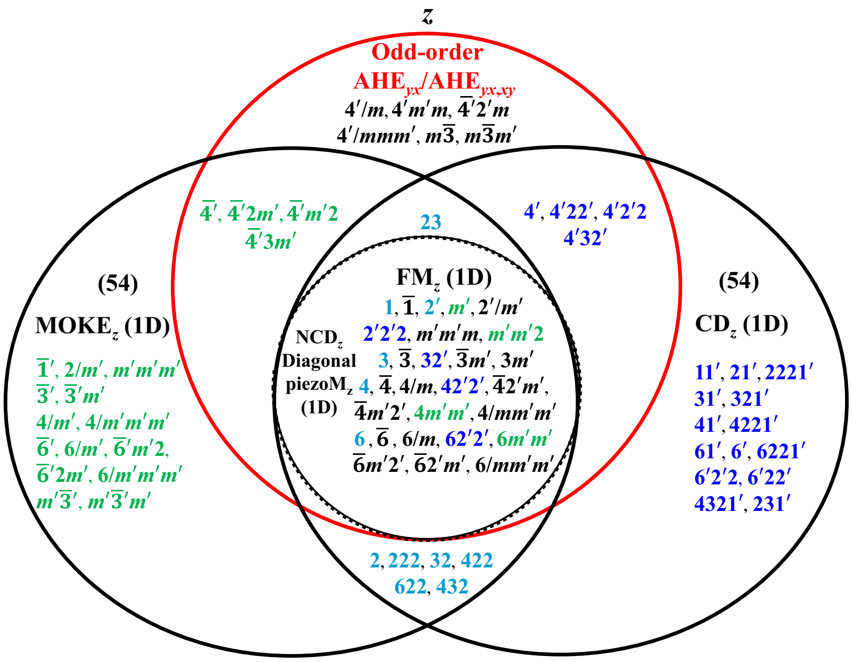


**Fig. 2 Magnetic point groups for various ferromagnetism-like phenomena along *z*.** Odd-order $AHE_{yx}$ is expected to be identical to Odd-order $AHE_{xy}$, except for the possible sign difference. Green: MPGs of diagonal linear magnetoelectric effect; Blue: MPGs of chiral point group; Turquoise: MPGs of linear magnetoelectric effect and chirality.

means an induced voltage difference and h/c (hot/cold) means an induced thermal gradient, accumulated on off-diagonal surfaces). In terms of symmetry, there is little difference among these four types of Hall effects, so, for example, the existence of non-zero AHE means the presence of non-zero anomalous Nernst effect. With this multi-faceted nature of Hall-type effect, it is imperative to find the accurate relationship among all different kinds of Hall-type effects, and also the requirements to have non-zero values of various Hall-type effects.

From our SOS analysis, we can tell a certain phenomenon is a zero, odd-order, or even-order effect. Herein, we will discuss the requirement of broken symmetries for odd-order anomalous Hall effects. We can have these transformations for the experimental setup for AHE measurements in Fig. 1e–h: (e) ↔ (e) by $\mathbf{M_z}$, $\mathbf{M_x{\otimes}T}$, and $\mathbf{R_y{\otimes}T}$; (e) ↔ (h) by **I**, $\mathbf{R_z}$, $\mathbf{M_y{\otimes}T}$, and $\mathbf{R_x{\otimes}T}$; (e) ↔ (f) by $\mathbf{M_y}$, $\mathbf{R_x}$, $\mathbf{I{\otimes}T}$, and $\mathbf{R_z{\otimes}T}$; (e) ↔ (g) by **T**, $\mathbf{M_x}$, $\mathbf{R_y}$, and $\mathbf{M_z{\otimes}T}$. Thus, Odd-order $AHE_{yx}$ means Odd-order AHE with current along *x* and Hall voltage along *y* in Fig. 1a, and the experimental setup to measure odd-order $AHE_{yx}$ has unbroken $[\mathbf{1,I,M_z,R_z,M_x{\otimes}T,M_y{\otimes}T,R_x{\otimes}T,R_y{\otimes}T}]$ and broken $\{\mathbf{I{\otimes}T,T,M_x,M_y,R_x,R_y,C_{3x},M_z{\otimes}T,R_z{\otimes}T}\}$. Now, any specimens having SOS with the above experimental setup will show Odd-order $AHE_{yx}$ when they have broken $\{\mathbf{I{\otimes}T,T,M_x,M_y,R_x,R_y,C_{3x},M_z{\otimes}T,R_z{\otimes}T}\}$. The rest independent ones can be either broken or unbroken. For example, for broken {**I**}, Odd-order AHE of the original domain is the same as that of the domain after space inversion. Emphasize that the requirements for anomalous Ettingshausen, anomalous Nernst, and anomalous thermal Hall effects are identical to those for AHE. It turns out that all ferromagnetic point groups[23,41] can have non-zero net magnetic moments. These MPGs display a symmetry pattern involving broken $\{\mathbf{I{\otimes}T,T,M_x,M_y,R_x,R_y,C_{3x},C_{3y}}\}$ with free rotation along *z* when the net magnetic moments align along the *z*-axis, or broken $\{\mathbf{I{\otimes}T,T,M_y,M_z,R_y,R_z,C_{3y},C_{3z}}\}$ with free rotation along *x* when the net magnetic moments are along *x*, or broken $\{\mathbf{I{\otimes}T,T,M_x,M_z,R_x,R_z,C_{3x},C_{3z}}\}$ with free rotation along *y* when the net magnetic moments are along *y* – the relevant MPGs are listed in Figs. 2–4.

As discussed earlier, all magnetic states in Fig. 1a–d belong to ferromagnetic point groups, so do exhibit Odd-order AHE. Since all magnetic states in Fig. 1(a–d) do accompany non-zero magnetic moments, the AHEs are, in fact, linear with applied electric current. MPGs for Odd-order $AHE_{yx}$, requiring broken $\{\mathbf{I{\otimes}T,T,M_x,M_y,R_x,R_y,C_{3x},M_z{\otimes}T,R_z{\otimes}T}\}$, and those for Odd-order $AHE_{yx,xy}$, requiring broken $\{\mathbf{I{\otimes}T,T,M_{xy},M_{yx},R_{xy},R_{yx},C_{3\text{-}xy},M_z{\otimes}T,R_z{\otimes}T}\}$, are listed in Fig. 2. MPGs for Odd-order $AHE_{zy}$, requiring broken $\{\mathbf{I{\otimes}T,T,M_y,M_z,R_y,R_z,C_{3y},M_x{\otimes}T,R_x{\otimes}T}\}$, and those for Odd-order $AHE_{zx}$, requiring broken $\{\mathbf{I{\otimes}T,T,M_x,M_z,R_x,R_z,C_{3x},M_y{\otimes}T,R_y{\otimes}T}\}$, are listed in Figs. 3 and 4, respectively. In all ferromagnetic point groups that can have non-zero net moments along *z* (*x* or *y*), Odd-order $AHE_{yx}$ ($AHE_{zy}$ or $AHE_{zx}$) is the same as Odd-order $AHE_{xy}$ ($AHE_{yz}$ or $AHE_{xz}$) except their sign difference (i.e. they are anti-symmetric).

However, there are three types of non-ferromagnetic point groups, which allow Odd-order AHE; (1) MPGs of $C_{3z}$ can have Odd-order $AHE_{zx}$ or $AHE_{zy}$ with broken $\{\mathbf{I{\otimes}T,T,M_z,M_y,R_z,R_y,C_{3y},M_x{\otimes}T,R_x{\otimes}T}\}$, but they have zero Odd-order $AHE_{xz}$ or $AHE_{yz}$ due to the unbroken $C_{3z}$: the examples are 3, $\bar{3}$, 32, 3*m*, $\bar{3}m$, 6′, $\bar{6}$′, 6′/*m*′, 6′22′, 6′*mm*′, $\bar{6}$′*m*2′, 6′/*m*′*mm*′ for Odd-order $AHE_{zy}$, and 3, $\bar{3}$, 32′, 3*m*′, $\bar{3}m$′, 6′, $\bar{6}$′, 6′/*m*′, $\bar{6}$′*m*′2 for Odd-order $AHE_{zx}$. (2) MPGs of $\mathbf{C_{4z}{\otimes}T}$ or $\mathbf{C_{4z}{\otimes}I{\otimes}T}$ can have Odd-order $AHE_{yx}$ and Odd-order $AHE_{xy}$ with broken $\{\mathbf{I{\otimes}T,T,M_x,M_y,R_x,R_y,C_{3x},C_{3y},M_z{\otimes}T,R_z{\otimes}T}\}$: the examples are 4′, $\bar{4}$′, 4′/*m*, 4′2′2, 4′*m*′*m*, $\bar{4}$′2′*m*, $\bar{4}$′*m*′2, 4′/*mm*′*m*. These MPGs are truly antiferromagnetic without any net magnetic moment but can exhibit odd-order AHE. All of these MPGs do have unbroken 4′ or $\bar{4}$′, so the odd-order AHEs in these point groups are associated with symmetric tensors, unlike antisymmetric tensors for odd-order AHEs in ferromagnetic space groups. For example, for $\bar{4}$′ point group, $(+\boldsymbol{J_x}{+}\boldsymbol{E_y})$ becomes $(+\boldsymbol{J_y}{+}\boldsymbol{E_x})$ under $\bar{4}$′, while the point group is invariant, so the relevant conductivity tensor components are symmetric. These Odd-order AHEs in truly antiferromagnetic states occur without non-zero magnetic moment, so must be high-order effects. High odd-order AHEs with symmetric tensors have never been reported and will be an exciting research direction. (3) Cubic MPGs allow Odd-order $AHE_{yx,xy}$ as well as Odd-order $AHE_{xy,yx}$: 23, *m*$\bar{3}$, 4′32′, $\bar{4}$′3*m*′, *m*$\bar{3}$*m*′.

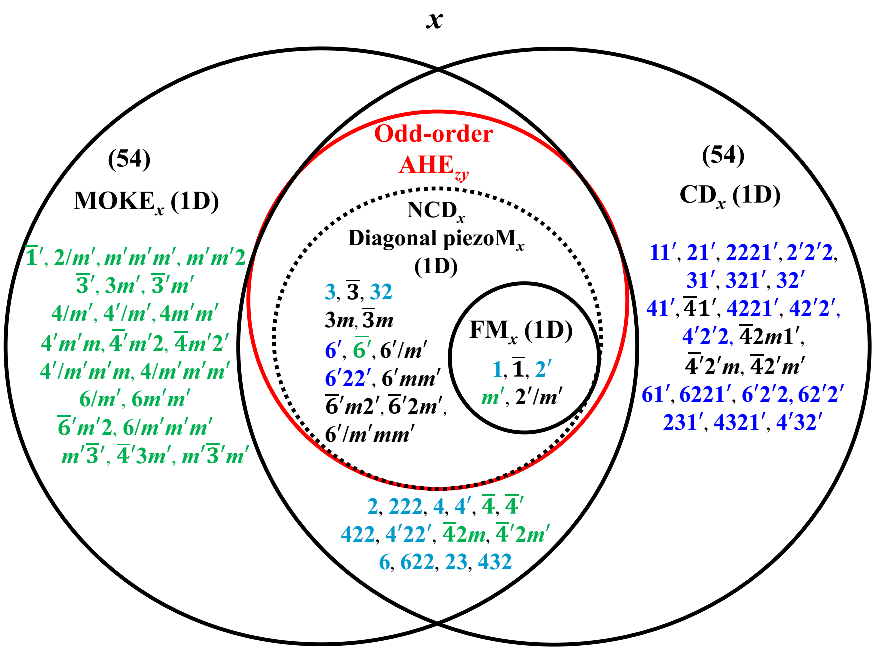


**Fig. 3 Magnetic point groups for various ferromagnetism-like phenomena along *x*.** Only in ferromagnetic point groups, Odd-order AHE$_{zy}$ is expected to be identical to Odd-order AHE$_{yz}$, except for the possible sign difference. Green: MPGs of diagonal linear magnetoelectric effect; Blue: MPGs of chiral point group; Turquoise: MPGs of both.

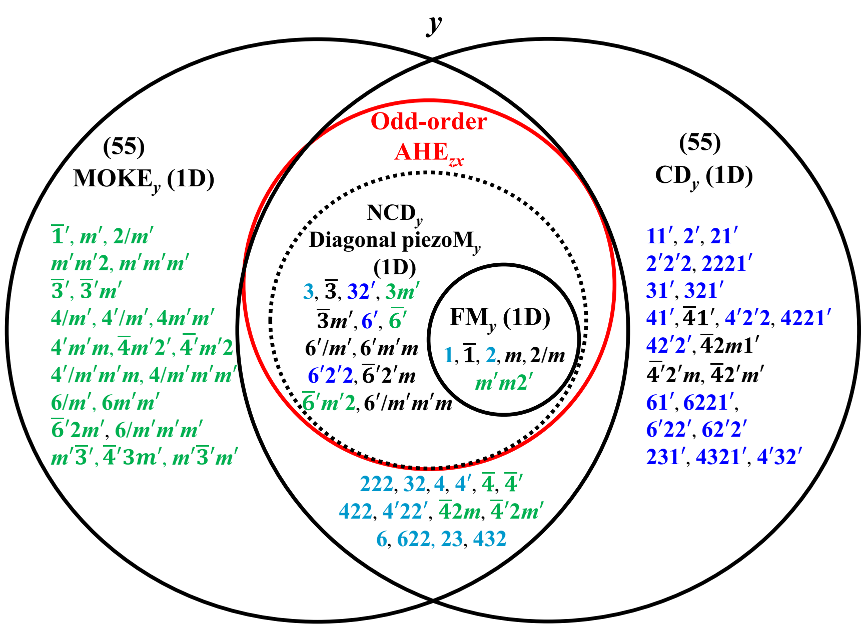


**Fig. 4 Magnetic point groups for various ferromagnetism-like phenomena along *y*.** Only in ferromagnetic point groups, Odd-order AHE$_{zx}$ is expected to be identical to Odd-order AHE$_{xz}$, except for the possible sign difference. Green: MPGs of diagonal linear magnetoelectric effect; Blue: MPGs of chiral point group; Turquoise: MPGs of both.

Note that those truly antiferromagnetic states mentioned above were omitted[20] from the list of MPGs exhibiting a Hall-vector in antiferromagnetic states in Ref. [20]. Furthermore, despite our symmetry requirements indicating their prohibition, MPGs *mmm*, 4/*mmm*, and 6/*mmm* were identified[42] as possessing 3$^{rd}$-order AHE responses driven by Berry curvature multipoles in Ref. [42].

It turns out that this Odd-order AHE corresponds to Off-diagonal even-order current-induced magnetization. When we consider the experimental setup for measuring magnetization along z induced in an even-order by current along *x*, we can readily find out that the relevant requirement for non-zero Off-diagonal even-order current-induced magnetization is broken $\{I\otimes T, T, M_x, M_y, R_x, R_y, C_{3x}, M_z\otimes T, R_z\otimes T\}$, which is identical with the requirement for Odd-order AHE$_{yx}$. Thus, we can conclude that Odd-order AHE results from Off-diagonal even-order current-induced magnetization. Zeroth-order current-induced magnetization is considered the cause of Linear AHE in ferromagnetic point groups with non-zero net magnetization in the presence of no current. Linear AHE can exist only in materials whose magnetic point groups belong to the ferromagnetic point group, which is always associated with non-zero net magnetic moments. In other words, there is absolutely no difference between the requirement for non-zero linear AHE and that for non-zero net magnetic moment in terms of symmetry. However, our symmetry argument cannot tell if the linear AHE effect is solely due to the net magnetic moment or not, and recent theories predict that the antiferromagnetic part of those magnetic point groups belonging to the ferromagnetic point group can be responsible for large linear AHE[7,14,21]. In any case, the 180° flipping of the net magnetic moment in any of those magnets by external magnetic fields is expected to result in the flipping of the entire antiferromagnetic vector and the sign change of linear AHE, even if the net magnetic moment is tiny. Note that ***k*** *(or **J**)* can represent electric current, light propagation as well as any constant currents such as phonon or magnon motions. Therefore, for example, phonons in any Odd-order AHE systems can accompany induced even-order magnetization that is perpendicular to the phonon ***k***. These phonons can be referred to as 'magnetic phonons'.

We emphasize that our SOS approach can tell if a certain phenomenon is zero, non-zero odd-order, or non-zero even-order effect, and broken {**I⊗T,T,M**$_x$**,M**$_y$**,R**$_x$**,R**$_y$**,C**$_{3x}$**,M**$_z$**⊗T,R**$_z$**⊗T**} is, in fact, the requirement for Odd-order AHE. Recently, the concept of altermagnetism was introduced: their ordered spins are truly antiferromagnetic, but can exhibit, for example, non-zero linear AHE due to orbital magnetism through Berry curvature[20,43,44]. However, it turns out that all those altermagnets, showing linear AHE discussed so far, such as MnTe and $RuO_2$ thin films[20,21] belong to ferromagnetic point groups.

## SYMMETRY OF PIEZOMAGNETISM

Piezoelectricity is the phenomenon of induced polarization, i.e., voltage gradient, with external stress. Similarly, piezomagnetism is the phenomenon of induced net magnetic moment with external stress, and there can exist Diagonal or Off-diagonal piezomagnetism. The experimental setup for Diagonal piezomagnetism along *z*, which is 1D, has broken {**I⊗T,T,M**$_x$**,M**$_y$**,R**$_x$**,R**$_y$} and unbroken [**1,I,M**$_z$**,R**$_z$], and thus has broken {**I⊗T,T,M**$_x$**,M**$_y$**,R**$_x$**,R**$_y$} with free rotation along *z*. MPGs for Diagonal piezomagnetism along *z*, requiring broken {**I⊗T,T,M**$_x$**,M**$_y$**,R**$_x$**,R**$_y$} with free rotation along *z*, those for Diagonal piezomagnetism along *x*, requiring broken {**I⊗T,T,M**$_y$**,M**$_z$**,R**$_y$**,R**$_z$} with free rotation along *x*, and those for Diagonal piezomagnetism along *y*, requiring broken {**I⊗T,T,M**$_x$**,M**$_z$**,R**$_x$**,R**$_z$} with free rotation along *y*, are listed in Figs. 2, 3 and 4, respectively. For example, 'broken {**I⊗T,T,M**$_x$**,M**$_y$**,R**$_x$**,R**$_y$} with free rotation along *z*' is a subset of 'broken {**I⊗T,T,M**$_x$**,M**$_y$**,R**$_x$**,R**$_y$**,C**$_{3x}$**,C**$_{3y}$} with free rotation along *z*', which is the requirement for ferromagnetic point groups with magnetization along *z*.

Therefore, all ferromagnetic point groups do exhibit Diagonal piezomagnetism along the magnetization direction. The only difference between the requirement for, for example, Diagonal piezomagnetism along *x* and that for ferromagnetic point groups with magnetization along *x* is broken {**C**$_{3y}$**,C**$_{3z}$}, and this difference is due to the breaking of both **C**$_{3y}$ and **C**$_{3z}$ by external stress along *x* in the case of Diagonal piezomagnetism along *x*. **C**$_3$ symmetry is defined to be along *z*, all MPGs, showing Diagonal piezomagnetism along *z*, belong to ferromagnetic point groups, but all MPGs with **C**$_{3z}$, showing Diagonal piezomagnetism along *x or y*, do not belong to ferromagnetic point groups, as shown in Figs. 3 and 4. Breaking **C**$_{3z}$ by external stress is the essential part of the Diagonal piezomagnetism along *x or y* in MPGs with **C**$_{3z}$, which do not exhibit magnetization along *x* or *y* in zero strain.

Off-diagonal piezomagnetism$_{zx}$ with stress along *x* and induced magnetization along *z* has broken {**I⊗T,T,M**$_x$**,M**$_y$**,R**$_x$**,R**$_y$**,C**$_{3x}$**,M**$_z$**⊗T,R**$_z$**⊗T**} and unbroken [**1,I,M**$_z$**,R**$_z$**,R**$_x$**⊗T,R**$_y$**⊗T**], and thus has broken {**I⊗T,T,M**$_x$**,M**$_y$**,R**$_x$**,R**$_y$**,C**$_{3x}$**,M**$_z$**⊗T,R**$_z$**⊗T**}, which is, interestingly, identical with the requirement for Odd-order AHE$_{yx}$. We also remark that in any piezomagnets, electric fields can also induce magnetization, but this electromagnetic effect will be of even order, meaning that the sign of the electric fields does not affect the outcome. In terms of ferromagnetism and piezomagnetism, the magnetic point groups identified via our SOS approach overlap with those obtained from the standard tensorial approach[2,23].

## SYMMETRY OF CIRCULAR DICHROISM

An experimental setup to measure Circular Dichroism (CD) is shown in Fig. 1(i–k). Circular Dichroism[45] includes the Faraday effect[46], natural optical activity, and Circular PhotoGalvanic Effect (CPGE)[47,48]. Figure 1(i, j) are linked through {**I⊗T,M**$_z$**⊗T,M**$_x$**,M**$_y$}, but each setup is invariant under [**1, I, M**$_z$**, R**$_x$**⊗T, R**$_y$**⊗T**] with any spatial rotation around *z*. Thus, this setup has broken {**I⊗T,M**$_x$**,M**$_y$} with any spatial rotation around *z* is required to have CD along *z* (CD$_z$). MPGs for CD$_z$, requiring broken {**I⊗T,M**$_x$**,M**$_y$}, those for CD$_x$, requiring broken {**I⊗T,M**$_y$**,M**$_z$}, and those for CD$_y$, requiring broken {**I⊗T,M**$_x$**,M**$_z$} are shown in Figs. 2, 3, and 4, respectively. Emphasize that for this symmetry consideration, we allow any spatial rotation around *z* freely. The broken-symmetry requirement for CD is a subset of those for Odd-order AHE, except that free rotations should be allowed for the symmetry consideration for CD. Thus, most of MPGs for non-zero Odd-order AHE, except $4'/m$, $4'm'm$, $\bar{4}'2'm$, $4'/mmm'$, $m\bar{3}$, $m\bar{3}m'$, $\bar{4}'$, $\bar{4}'2m'$,$\bar{4}'m2'$, $\bar{4}'3m'$ for Odd-order AHE$_{yx}$, allow CD$_z$. In the case of all ferromagnetic point groups, which is a part of MPGs for Odd-order AHE, CD is always along the magnetization direction.

Now, CD can be nonreciprocal if all of {**T,R**$_x$**,R**$_y$**,C**$_{3x}$**,C**$_{3y}$} are broken additionally since any of {**T,R**$_x$**,R**$_y$} can link Fig. 1i and Fig. 1k in the condition of any free rotations along *z*. Thus, the requirement for Nonreciprocal CD (NCD) along *z* is broken {**I⊗T,T,M**$_x$**,M**$_y$**,R**$_x$**,R**$_y$} with free rotation along *z*, which is identical to the requirement for Diagonal piezomagnetism along *z*. Thus, all MPGs for Diagonal piezomagnetism along one direction do exhibit NCD along the direction. All ferromagnetic point groups do exhibit NCD along the magnetization direction, which is associated with the Faraday effect. Note that breaking **C**$_{3z}$ by external stress, discussed in the above section, becomes also relevant for CD, since light propagation itself can also break **C**$_{3z}$. The following example illustrates how NCD can be linked with Diagonal piezomagnetism in nonferromagnetic point groups. Non-ferromagnetic MPGs, such as 32, 3*m*, and $\bar{3}m$, should exhibit NCD$_x$ with zero NCD$_{y\text{ or }z}$, and they also exhibit Diagonal piezomagnetism along *x* (piezo***M***$_x$). Diagonal piezo***M***$_x$ is the same as Diagonal even-order (e.g. 2$^{nd}$-order) current (light propagation or electric current)-induced ***M***, and this induced ***M*** can result in NCD.

Both space-inversion and time-reversal symmetries are broken in 32 and 3*m*, and their space-inversion domains do exhibit the identical NCD$_x$, but their time-reversal domains should display the opposite NCD$_x$. We emphasize that light-induced ***M*** can result in reciprocal CD as well as NCD. For example, reciprocal CD (i.e., natural optical activity) occurs in chiral point groups, and light propagation in chiral materials does induce ***M*** along the light propagation direction in a linear fashion, which, in turn, results in ***M***-induced CD[49]. Since the induced ***M*** flips its sign when the light propagation direction flips by 180° (i.e. ***M*** is induced in a linear fashion), this CD effect is reciprocal. In other words, natural optical activity in chiral materials can be understood in terms of the Faraday effect due to light-induced ***M***.

## SYMMETRY OF MAGNETO-OPTICAL KERR EFFECT (MOKE)

The experimental setup to measure the non-zero Magneto-Optical Kerr Effect (MOKE), i.e. the light-polarization rotation effect of reflected linearly-polarized light, is shown in Fig. 1l, m. First, we note that this experimental setup is also invariant under any spatial rotations around $z$, so we can ignore or freely allow any rotations around $z$ for symmetry considerations. The MOKE setup has broken $\{\mathbf{T},\mathbf{M}_x,\mathbf{M}_y\}$, so the requirement for MOKE along $z$ ($\mathrm{MOKE}_z$) is broken $\{\mathbf{T},\mathbf{M}_x,\mathbf{M}_y\}$ with freely-allowed rotations around $z$. MPGs for $\mathrm{MOKE}_z$, requiring broken $\{\mathbf{T},\mathbf{M}_x,\mathbf{M}_y\}$ with free rotation around $z$, those for $\mathrm{MOKE}_x$, requiring broken $\{\mathbf{T},\mathbf{M}_y,\mathbf{M}_z\}$ with free rotation around $z$, and those for $\mathrm{MOKE}_y$, requiring broken $\{\mathbf{T},\mathbf{M}_x,\mathbf{M}_z\}$ with free rotation around $z$, are summarized in Figs. 2, 3 and 4, respectively. Note that, for example, in tetragonal point groups, $\mathbf{M}_x$ can be different from $\mathbf{M}_{xy}$, and broken $\{\mathbf{T},\mathbf{M}_x,\mathbf{M}_y\}$ with freely-allowed rotations around $z$ means broken $\{\mathbf{T},\mathbf{M}_x,\mathbf{M}_y,\mathbf{M}_{xy},\mathbf{M}_{yx}\}$ for those tetragonal point groups. Certainly, all ferromagnetic point groups have broken $\{\mathbf{T},\mathbf{M}_x,\mathbf{M}_y\}$, so they exhibit MOKE.

It turns out that the requirement for diagonal linear magnetoelectric effects along $z$ is broken $\{\mathbf{T},\mathbf{I},\mathbf{M}_x,\mathbf{M}_y,\mathbf{R}_x\otimes\mathbf{T},\mathbf{R}_y\otimes\mathbf{T}\}$ with free rotation along $z$, which requires more broken symmetries than $\mathrm{MOKE}_z$, so all linear magnetoelectrics along $z$ do exhibit $\mathrm{MOKE}_z$. Our symmetry analysis has revealed that MPGs permitting the MOKE effect extend beyond the confines of the 31 ferromagnetic point groups documented in the literature[50]. Figures 2–4 vividly illustrate non-ferromagnetic MPG examples for the MOKE effect, encompassing those associated with linear magnetoelectric properties (highlighted in green and turquoise), as well as MPGs characterized by diagonal piezomagnetism (central dotted circles) and chiral point groups (highlighted in blue and turquoise). The phenomena of MOKE in all linear magnetoelectrics can be considered as a result of magnetization induced by the presence of a surface in diagonal linear magnetoelectrics, since the presence of a surface is necessary for MOKE and any surface of all diagonal linear magnetoelectrics can have surface magnetization[51].

Figures 2–4 provide a concise overview of ferromagnetism-like phenomena in three principal directions: $z$, $x$, and $y$ with the required broken symmetries presented in Table 1. The symmetry criteria of Circular Dichroism (CD) and Magneto-Optical Kerr Effect (MOKE) are shown to be interchangeable through the $\mathbf{I}\otimes\mathbf{T}\leftrightarrow\mathbf{T}$ symmetry transformation. Note that $\mathbf{I}\otimes\mathbf{T}\leftrightarrow\mathbf{T}$ accompanies, for example, $\mathbf{M}_x\otimes\mathbf{T}=\mathbf{R}_x\otimes\mathbf{I}\otimes\mathbf{T}\leftrightarrow\mathbf{R}_x\otimes\mathbf{T}$. $\mathrm{CD}_z$ requires the lack of $\{\mathbf{I}\otimes\mathbf{T},\mathbf{M}_x,\mathbf{M}_y\}$ symmetries with any spatial rotation around $z$, which can be transformed into $\{\mathbf{T},\mathbf{M}_x,\mathbf{M}_y\}$ for $\mathrm{MOKE}_z$. Figures 2–4 visually represent the interconnection. Figure 2 illustrates the same number, 54, MPGs, enclosed within the large $\mathrm{CD}_z$ and $\mathrm{MOKE}_z$ circles, respectively, while also showing the same number, 34, of MPGs at their intersection with odd-order $\mathrm{AHE}_{yx}$. Figures 3 and 4 similarly reflect symmetrical patterns for $\mathrm{CD}_x$ & $\mathrm{MOKE}_x$ (Fig. 3) and $\mathrm{CD}_y$ & $\mathrm{MOKE}_y$ (Fig. 4). This observation reveals the concept that Circular Dichroism (CD) and Magneto-Optical Kerr Effect (MOKE) can be viewed as conjugate phenomena in the context of underlying symmetry.

## CANDIDATE MATERIALS

Using Figs. 2–4, one can readily identify potential materials suitable for measuring the various phenomena we have discussed. Materials belonging to thirty-one ferromagnetic point groups (1, $\bar{1}$, 2, 2′, $m$, $m'$, 2/$m$, 2′/$m'$, 2′2′2, $m'm'm$, $m'm'$2, $m'm$2′, 4, $\bar{4}$, 4/$m$, 42′2′, 4$m'm'$, $\bar{4}$2′$m'$, 4/$mm'm'$, 3, $\bar{3}$, 32′, 3$m'$, $\bar{3}m'$, 6, $\bar{6}$, 6/$m$, 62′2′, 6$m'm'$, $\bar{6}m'$2′, 6/$mm'm'$) can exhibit all relevant phenomena. As we have discussed, these materials include seemingly-antiferromagnetic magnets such as $Mn_3$(Sn,Ge,Ga,Rh,Ir,Pt), as shown in Fig. 1a, b and d and the so-called altermagnets such as MnTe and $RuO_2$ with the MPG $m'm'm$[20,21]. Another examples are metallic cubic $Pd_3Mn$[52] and insulating $NaMnFeF_6$[53] forming in ferromagnetic 32′ with unbroken $[\mathbf{C}_{3z},\mathbf{R}_x\otimes\mathbf{T}]$. The 32′ point group, allowing all of these phenomena, e.g. $\mathrm{magnetization}_z$, Odd-order $\mathrm{AHE}_{yx}$, Odd-order $\mathrm{AHE}_{xy}$, Odd-order $\mathrm{AHE}_{zx}$, $\mathrm{NCD}_{y\ or\ z}$, Diagonal $\mathrm{piezomagnetism}_{y\ or\ z}$, and $\mathrm{MOKE}_{y\ or\ z}$, so $Pd_3Mn$ and $NaMnFeF_6$ can be studied for these phenomena. Note that since magnetization of 32′ is along $z$, so

**Table 1.** Required broken symmetries and relevant MPGs for certain measurables or phenomena.

| Measurables | Required broken symmetries |
|---|---|
| **Non-zero magnetization$_z$ (FR$_z$)** | $\{\mathbf{I}\otimes\mathbf{T},\mathbf{T},\mathbf{M}_x,\mathbf{M}_y,\mathbf{R}_x,\mathbf{R}_y,\mathbf{C}_{3x},\mathbf{C}_{3y}\}$ |
| • **Ferromagnetic MPGs with $M_z$:** 1, $\bar{1}$, 2′, $m'$, 2′/$m'$, 2′2′2, $m'm'$2, $m'm'm$, 3, $\bar{3}$, 32′, 3$m'$, $\bar{3}m'$, 4, $\bar{4}$, 4/$m$, 42′2′, 4$m'm'$, $\bar{4}$2′$m'$, $\bar{4}m'$2′, 4/$mm'm'$, 6, $\bar{6}$, 6/$m$, 62′2′, 6$m'm'$, $\bar{6}$2′$m'$, $\bar{6}m'$2′, 6/$mm'm'$ | |
| **Diagonal piezomagnetism$_z$ (Nonreciprocal optical activity) (FR$_z$)** | $\{\mathbf{I}\otimes\mathbf{T},\mathbf{T},\mathbf{M}_x,\mathbf{M}_y,\mathbf{R}_x,\mathbf{R}_y\}$ |
| • **Ferromagnetic MPGs with $M_z$:** 1, $\bar{1}$, 2′, $m'$, 2′/$m'$, 2′2′2, $m'm'$2, $m'm'm$, 3, $\bar{3}$, 32′, 3$m'$, $\bar{3}m'$, 4, $\bar{4}$, 4/$m$, 42′2′, 4$m'm'$, $\bar{4}$2′$m'$, $\bar{4}m'$2′, 4/$mm'm'$, 6, $\bar{6}$, 6/$m$, 62′2′, 6$m'm'$, $\bar{6}$2′$m'$, $\bar{6}m'$2′, 6/$mm'm'$ | |
| **Odd-order AHE$_{yx}$** | $\{\mathbf{I}\otimes\mathbf{T},\mathbf{T},\mathbf{M}_x,\mathbf{M}_y,\mathbf{R}_x,\mathbf{R}_y,\mathbf{C}_{3x},\mathbf{M}_z\otimes\mathbf{T},\mathbf{R}_z\otimes\mathbf{T}\}$ |
| • **Ferromagnetic MPGs with $M_z$:** 1, $\bar{1}$, 2′, $m'$, 2′/$m'$, 2′2′2, $m'm'$2, $m'm'm$, 3, $\bar{3}$, 32′, 3$m'$, $\bar{3}m'$, 4, $\bar{4}$, 4/$m$, 42′2′, 4$m'm'$, $\bar{4}$2′$m'$, $\bar{4}m'$2′, 4/$mm'm'$, 6, $\bar{6}$, 6/$m$, 62′2′, 6$m'm'$, $\bar{6}$2′$m'$, $\bar{6}m'$2′, 6/$mm'm'$<br>• 4′, $\bar{4}'$, 4′/$m$, 4′2′2, 4′$m'm$, $\bar{4}'m'$2, $\bar{4}'$2′$m$, 4′/$mm'm$<br>• 23, $m\bar{3}$, 4′32′, $\bar{4}'$3$m'$, $m\bar{3}m'$ for current along $xy$ or $yx$ | |
| **Circular Dichroism$_z$ (FR$_z$)** | $\{\mathbf{I}\otimes\mathbf{T},\mathbf{M}_x,\mathbf{M}_y\}$ |
| • Ferromagnetic MPGs with $M_z$: $\bar{1}$, $m'$, 2′/$m'$, $m'm'$2, $m'm'm$, $\bar{3}$, 3$m'$, $\bar{3}m'$, $\bar{4}$, 4/$m$, 4$m'm'$, $\bar{4}$2′$m'$, $\bar{4}m'$2′, 4/$mm'm'$, $\bar{6}$, 6/$m$, 6$m'm'$, $\bar{6}$2′$m'$, $\bar{6}m'$2′, 6/$mm'm'$<br>• Chiral MPGs: 11′, 2, 21′, 222, 2221′, 41′, 4′, 422, 4221′, 4′2′2, 4′22′, 31′, 32, 321′, 61′, 6′, 622, 6221′, 6′22′, 6′2′2, 23, 231′, 432, 4321′, 4′32′<br>• $M_z$ & Chiral: 1, 2′, 2′2′2, 4, 42′2′, 3, 32′, 6, 62′2′ | |
| **MOKE$_z$ (FR$_z$)** | $\{\mathbf{T},\mathbf{M}_x,\mathbf{M}_y\}$ |
| • Ferromagnetic MPGs with $M_z$: $\bar{1}$, 2′/$m'$, 2′2′2, $m'm'm$, $\bar{3}$, 32′, 3$m'$, $\bar{3}m'$, $\bar{4}$, 4/$m$, 42′2′, $\bar{4}$2′$m'$, $\bar{4}m'$2′, 4/$mm'm'$, $\bar{6}$, 6/$m$, 62′2′, $\bar{6}$2′$m'$, $\bar{6}m'$2′, 6/$mm'm'$<br>• Linear magnetoelectrics: $\bar{1}$, 2, 2/$m'$, $m'm'm'$, 222, $\bar{3}'$, $\bar{3}'m'$, 32, $\bar{4}'$, 4/$m'$, 422, $\bar{4}'$2$m'$, $\bar{4}'m'$2, 4/$m'm'm'$, $\bar{6}'$, 6/$m'$, 622, $\bar{6}'$2$m'$, $\bar{6}'m'$2, 6/$m'm'm'$, 23, $m'\bar{3}'$, 432, $\bar{4}'$3$m'$, $m'\bar{3}'m'$<br>• $M_z$ & ME$_z$: 1, 2′, $m'$, $m'm'$2, 3, 4, 4$m'm'$, 6, 6$m'm'$ | |

The subscriptions of $x$, $y$ and $z$ mean the relevant orientations: for example, Odd-order $\mathrm{AHE}_{yx}$ means current along $x$ and Hall voltage along $y$, and Diagonal $\mathrm{piezomagnetism}_z$, Circular $\mathrm{Dichroism}_z$, and $\mathrm{MOKE}_z$ are along $z$. Note that Odd-order $\mathrm{AHE}_{yx}$ = Odd-order $\mathrm{AHE}_{xy}$ except sign in all ferromagnetic point groups. We emphasize that when we consider broken symmetries, we ignore or freely allow any rotations around the 1D direction for 1D phenomena such as Diagonal $\mathrm{piezomagnetism}_z$, Circular $\mathrm{Dichroism}_z$, and $\mathrm{MOKE}_z$ ($\mathrm{FR}_z$ means free rotation around $z$). For example, MPG $\bar{4}$1′ has unbroken $\mathbf{T}$ and broken $\mathbf{I}$, but $\mathbf{I}\otimes\mathbf{C}_{4z}$ is unbroken, so $\mathbf{I}\otimes\mathbf{T}$ is unbroken with $\mathrm{FR}_z$ and it cannot exhibit Circular $\mathrm{Dichroism}_z$; however, $\bar{4}$1′ can exhibit Circular $\mathrm{Dichroism}_{\mathbf{x}\ \mathbf{or}\ \mathbf{y}}$.

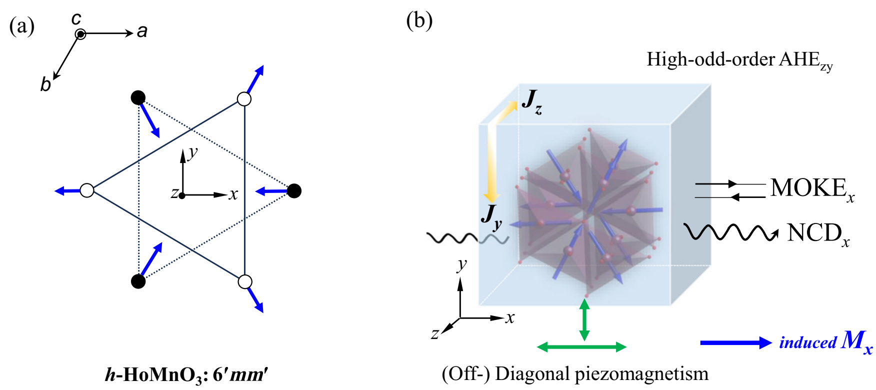


**Fig. 5 Various phenomena in MPG 6′mm′. a** A schematic of antiferromagnetic order in the Mn trimerized triangular layers of polar $h$-$HoMoO_3$. The B1 phase of the MPG 6′mm′ appears below 70 K. **b** A schematic of the sample configuration for measurements including high-odd-order AHE$_{zy}$, MOKE$_x$, NCD$_x$, off-diagonal piezomagnetism$_{xy}$, and Diagonal piezomagnetism$_x$. $J_y$ the applied electric current and $J_z$ the Hall current. Green double arrows denote stress forces.

Odd-order AHE$_{yx}$, Odd-order AHE$_{xy}$, NCD$_z$, Diagonal piezomagnetism$_z$ and MOKE$_z$ are entirely expected; however, they can also exhibit Odd-order AHE$_{zx}$, NCD$_y$, Diagonal piezomagnetism$_y$ and MOKE$_y$, even though magnetization along $y$ is zero. These off-magnetization-direction phenomena have never been observed.

Emphasize that the current for AHE can be electric current or other propagating quasiparticles such as thermal current, propagating lights, magnons and phonons. As discussed earlier, Odd-order AHE, associated with symmetric tensors, can occur in true antiferromagnets in the MPGs of 4′, $\bar{4}$′, 4′/m, 4′2′2 (or 4′22′), 4′m′m (or 4′mm′), $\bar{4}$′2′m, $\bar{4}$′m′2 ($\bar{4}$′2m′), 4′/mmm′. MPG of the magnetic ground state of $RuO_2$ in bulk form is 4′/mmm′[19], which does not belong to the ferromagnetic point group. Thus, high-odd-order AHE can be expected in $RuO_2$, which requires future experimental confirmation. The magnetic states of insulating $Er_2Ge_2O_7$ and $Pb(TiO)Cu_4(PO_4)_4$ are non-ferromagnetic 4′22′ with unbroken [$\mathbf{C_{4z}\otimes T, R_z, R_x, R_y, R_{xy}\otimes T, R_{yx}\otimes T}$], allowing Odd-order AHE$_{yx,xy}$, CD$_{x,\ y,\ xy,\ yx\ or\ z}$, and MOKE$_{x,\ y,\ xy\ or\ yx}$. Thus, it is imperative to measure Odd-order AHE$_{yx,xy}$, CD$_{x,\ y,\ xy,\ yx\ or\ z}$, and MOKE$_{x,\ y,\ xy\ or\ yx}$ in $Pb(TiO)Cu_4(PO_4)_4$ and $Er_2Ge_2O_7$. Note that this Odd-order AHE$_{yx,xy}$ can be observed as an anomalous thermal Hall effect in those insulating 4′22′ systems without any ferromagnetic moment.

Ferroelectric hexagonal $h$-$HoMnO_3$ adopts the $B_1$ magnetic state below 70 K, which corresponds to MPG 6′mm′[54,55]. Fig. 5a depicts the triangular configuration of spins in the $ab$-plane with MPG 6′mm′. MPG 6′mm′ allows Off-diagonal piezomagnetism$_{xy}$, Odd-order AHE$_{zy}$, Diagonal piezomagnetism$_x$, NCD$_x$, and MOKE$_x$ (Fig. 5b), all of which are the results of our SOS analysis and need to be experimentally verified. The antiferromagnetic state of $Fe_2Mo_3O_8$ also forms in the same MPG 6′mm′[56]. Note that when we have Diagonal odd-order (such as linear) piezomagnetism$_x$ and Off-diagonal odd-order (such as linear) piezomagnetism$_{xy}$, applying an electric field or current along $x$ or $y$ will induce magnetization along $x$, which is an even-order (such as quadratic) with applied electric field/current, so the sign change of applied electric field/current will not change the sign of induced magnetization. Finally, note that the MPG of $CsFeCl_3$[57] below $T_N = 4.7$ K is $\bar{6}$′m2′, while the point group of it above $T_N$ is centrosymmetric 6/mmm. $\bar{6}$′m2′ has unbroken [$\mathbf{C_{6z}\otimes I\otimes T, C_{3z}, M_x, R_y\otimes T, M_z\otimes T}$], so can exhibit Odd-order AHE$_{zy}$, NCD$_x$, Diagonal piezomagnetism$_x$, and MOKE$_x$. Thus, insulating $CsFeCl_3$ in a non-ferromagnetic point group with zero magnetization can exhibit NCD such as the Faraday effect, which has been always thought to be confined in ferromagnetic systems.

## CONCLUSION

Our SOS concept incorporates the symmetry relationship between the specimen and the experimental setup, encompassing measurable parameters and the sample environment, without considering local couplings or relevant tensorial terms. The SOS approach can tell if a certain measurable relevant to a particular phenomenon is zero, non-zero odd-order, or non-zero even-order of, for example, applied electric current. By employing this SOS approach, we have successfully identified all MPGs relevant for each of ferromagnetism-like phenomena, including magnetic attraction/repulsion, diagonal piezomagnetism, nonreciprocal circular dichroism (such as Faraday effect), odd-order (including linear) anomalous Hall effect, and magneto-optical Kerr effect. The ferromagnetism-like phenomena can manifest only in two ways: first, through non-zero magnetization in ferromagnetic point groups, where symmetry permits non-zero magnetization; and second, through magnetization induced by external perturbations such as electric current flow, light propagation, or stress. Undoubtedly, the categorized MPGs for each ferromagnetism-like phenomenon, along with our SOS approach, will serve as crucial guidance for future advancements in magnetism-related science and technology.

## DATA AVAILABILITY

All study data is included in the article.

Received: 24 May 2023; Accepted: 10 November 2023;
Published online: 05 December 2023

## REFERENCES

1. Newnham, R. E. Properties of materials anisotropy, symmetry, structure. 30–36, 122–146 (Oxford University Press, Oxford, 2005).
2. Birss, R. R. Symmetry and magnetism. 125–138 (North-Holland Pub. Co., Amsterdam, 1964).
3. Landau, L. D. & Lifshitz, E. M. Chapter V - Ferromegnetism and anti-ferromagnetism, in *Electrodynamics of Continuous Media* Vol. 8. (eds. L. D. Landau & E. M. Lifshitz) 130-179 (Pergamon, Amsterdam, 1984).
4. Erskine, J. L. & Stern, E. A. Calculation of the M23 magneto-optical absorption spectrum of ferromagnetic nickel. *Phys. Rev. B* **12**, 5016–5024 (1975).
5. Thole, B. T. et al. Experimental proof of magnetic x-ray dichroism. *Phys. Rev. B* **34**, 6529–6531 (1986).
6. Schtz, G. et al. Absorption of circularly polarized x rays in iron. *Phys. Rev. Lett.* **58**, 737–740 (1987).
7. Chen, H., Niu, Q. & Macdonald, A. H. Anomalous hall effect arising from non-collinear antiferromagnetism. *Phys. Rev. Lett.* **112**, 017205 (2014).

8. Katsufuji, T., Hwang, H. Y. & Cheong, S. W. Anomalous magnetotransport properties of $R_2Mo_2O_7$ near the magnetic phase boundary. *Phys. Rev. Lett.* **84**, 1998–2001 (2000).
9. Liu, J. & Balents, L. Anomalous Hall effect and topological defects in antiferromagnetic Weyl semimetals: $Mn_3Sn$/Ge. *Phys. Rev. Lett.* **119**, 087202 (2017).
10. Nagaosa, N., Sinova, J., Onoda, S., MacDonald, A. H. & Ong, N. P. Anomalous Hall effect. *Rev. Mod. Phys.* **82**, 1539–1592 (2009).
11. Ramos, R. et al. Anomalous Nernst effect of $Fe_3O_4$ single crystal. *Phys. Rev. B* **90**, 054422 (2014).
12. Sakai, A. et al. Giant anomalous Nernst effect and quantum-critical scaling in a ferromagnetic semimetal. *Nat. Phys.* **14**, 1119–1124 (2018).
13. Qiu, Z. Q. & Bader, S. D. Surface magneto-optic Kerr effect. *Rev. Sci. Instr.* **71**, 1243–1255 (2000).
14. Nakatsuji, S., Kiyohara, N. & Higo, T. Large anomalous Hall effect in a non-collinear antiferromagnet at room temperature. *Nature* **527**, 212–215 (2015).
15. Nayak, A. K. et al. Large anomalous Hall effect driven by a nonvanishing Berry curvature in the noncolinear antiferromagnet $Mn_3Ge$. *Sci. Adv.* **2**, e1501870 (2016).
16. Seki, T., Iguchi, R., Takanashi, K. & Uchida, K. Visualization of anomalous Ettingshausen effect in a ferromagnetic film: Direct evidence of different symmetry from spin Peltier effect. *Appl. Phys. Lett.* **112**, 152403 (2018).
17. Park et al. Magnetic excitations in non-collinear antiferromagnetic Weyl semimetal $Mn_3Sn$. *npj Quantum Mater.* **3**, 63 (2018).
18. Karplus, R. & Luttinger, J. M. Hall effect in ferromagnetics. *Phys. Rev.* **95**, 1154–1160 (1954).
19. Berlijn, T. et al. Itinerant antiferromagnetism in $RuO_2$. *Phys. Rev. Lett.* **118**, 077201 (2017).
20. Šmejkal, L. et al. Crystal time-reversal symmetry breaking and spontaneous Hall effect in collinear antiferromagnets. *Sci. Adv.* **6**, eaaz8809 (2020).
21. Gonzalez Betancourt, R. D. et al. Spontaneous anomalous Hall effect arising from an unconventional compensated magnetic phase in a semiconductor. *Phys. Rev. Lett.* **130**, 036702 (2023).
22. Cheong, S.-W. Trompe L'oeil Ferromagnetism. *npj Quantum Mater.* **5**, 37 (2020).
23. Schmid, H. Some symmetry aspects of ferroics and single-phase multiferroics. *J. Phys. Condens. Matter* **20**, 434201 (2008).
24. Chen, C. T., Sette, F., Ma, Y. & Modesti, S. Soft-x-ray magnetic circular dichroism at the L2,3 edges of nickel. *Phys. Rev. B* **42**, 7262–7265 (1990).
25. Lubashevsky, Y., Pan, L., Kirzhner, T., Koren, G. & Armitage, N. P. Optical birefringence and dichroism of cuprate superconductors in the THz regime. *Phys. Rev. Lett.* **112**, 147001 (2014).
26. Stephens, P. J. Magnetic circular dichroism. *Annu. Rev. Phys. Chem.* **25**, 201–232 (1974).
27. Schatz, P. N. & McCaffery, A. J. The Faraday effect. *Q. Rev. Chem. Soc.,* **23**, 552–584 (1969).
28. Higo, T. et al. Large magneto-optical Kerr effect and imaging of magnetic octupole domains in an antiferromagnetic metal. *Nat. Photon.* **12**, 73–78 (2018).
29. Cheong, S. W. SOS: symmetry operational similarity. *npj Quantum Mater.* **4**, 53 (2019).
30. Grimmer, H. General connections for the form of property tensors in the 122 Shubnikov point groups. *Acta Crystallogr. A* **47**, 226–232 (1991).
31. Shuvalov, L. A. Modern crystallography. IV. Physical properties of crystals. 1–46 (Springer England, 1989).
32. Neumann, F. E. *Vorlesungen über die Theorie der Elasticität der festen Körper und des Lichtäthers, gehalten an der Universität Königsberg von Dr. Franz Neumann. Hrsg. von Dr. Oskar Emil Meyer, mit Figuren im Text*. (B. G. Teubner, 1885).
33. Cheong, S.-W., Huang, F.-T. & Minhyong, K. Linking emergent phenomena and broken symmetries through one-dimensional objects and their dot/cross products. *Rep. Prog. Phys.* **85**, 124501 (2022).
34. Cheong, S.-W., Lim, S., Du, K., Huang, F.-T. & Permutable, S. O. S. Symmetry operational similarity. *npj Quantum Mater.* **6**, 58 (2021).
35. Matan, K. et al. Magnetic structure and high-field magnetization of the distorted kagome lattice antiferromagnet $Cs_2Cu_3SnF_{12}$. *Phys. Rev. B* **99**, 224404 (2019).
36. Feng, W., Guo, G.-Y., Zhou, J., Yao, Y. & Niu, Q. Large magneto-optical Kerr effect in noncollinear antiferromagnets $Mn_3X$ (X=Rh, Ir, Pt). *Phys. Rev. B* **92**, 144426 (2015).
37. Hall, E. H. On a new action of the magnet on electric currents. *Am. J. Math.* **2**, 287–292 (1879).
38. Kanazawa, N. et al. Large topological hall effect in a short-period helimagnet MnGe. *Phys. Rev. Lett.* **106**, 156603 (2011).
39. Neubauer, A. et al. Topological Hall effect in the a phase of MnSi. *Phys. Rev. Lett.* **102**, 186602 (2009).
40. Baltz, V. et al. Antiferromagnetic spintronics. *Rev. Mod. Phys.* **90**, 015005 (2018).
41. Gallego, S. V. et al. MAGNDATA: towards a database of magnetic structures. I. The commensurate case. *J. Appl. Crystallogr.* **49**, 1750–1776 (2016).
42. Zhang, C.-P., Gao, X.-J., Xie, Y.-M., Po, H. C. & Law, K. T. Higher-order nonlinear anomalous Hall effects induced by Berry curvature multipoles. *Phys. Rev. B* **107**, 115142 (2023).
43. Šmejkal, L., Sinova, J. & Jungwirth, T. Emerging research landscape of altermagnetism. *Phys. Rev. X* **12**, 040501 (2022).
44. Šmejkal, L., Sinova, J. & Jungwirth, T. Beyond conventional ferromagnetism and antiferromagnetism: a phase with nonrelativistic spin and crystal rotation symmetry. *Phys. Rev. X.* **12**, 031042 (2022).
45. Yokosuk, M. O. et al. Nonreciprocal directional dichroism of a chiral magnet in the visible range. *npj Quantum Mater.* **5**, 20 (2020).
46. Juraschek, D. M., Fechner, M., Balatsky, A. V. & Spaldin, N. A. Dynamical multiferroicity. *Phys. Rev. Mater.* **1**, 014401 (2017).
47. Ni, Z. et al. Linear and nonlinear optical responses in the chiral multifold semimetal RhSi. *npj Quantum Mater.* **5**, 96 (2020).
48. Belinicher, V. I. Space-oscillating photocurrent in crystals without symmetry center. *Phys. Lett. A* **66**, 213–214 (1978).
49. Furukawa, T., Shimokawa, Y., Kobayashi, K. & Itou, T. Observation of current-induced bulk magnetization in elemental tellurium. *Nat. Commun.* **8**, 954 (2017).
50. Yang, K. et al. Magneto-optical Kerr switching properties of $(CrI_3)_2$ and $(CrBr_3/CrI_3)$ bilayers. *ACS Appl. Electron*. *Mater* **2**, 1373–1380 (2020).
51. Du, K. et al. Topological surface magnetism and Néel vector control in a magnetoelectric antiferromagnet. *npj Quantum Mater.* **8**, 17 (2023).
52. Önnerud, P., Andersson, Y., Tellgren, R. & Nordblad, P. The magnetic structure of ordered cubic $Pd_3Mn$. *J. Solid State Chem.* **128**, 109–114 (1997).
53. Courbion, G. & Leblanc, M. The magnetic structure of $NaMnFeF_6$. *J. Magn. Magn. Mater.* **74**, 158–164 (1988).
54. Brown, P. J. & Chatterji, T. Neutron diffraction and polarimetric study of the magnetic and crystal structures of $HoMnO_3$ and $YMnO_3$. *J. Phys. Condens. matter* **18**, 10085–10096 (2006).
55. Ratcliff, W., Lynn, J. W., Kiryukhin, V., Jain, P. & Fitzsimmons, M. R. *npj Quantum Mater.* **1**, 16003 (2016).
56. Bertrand, D. & Kerner-Czeskleba, H. Étude structurale et magnétique de molybdates d'éléments de transition. *J. Phys.* **36**, 379–390 (1975).
57. Hayashida, S. et al. Pressure-induced quantum phase transition in the quantum antiferromagnet $CsFeCl_3$. *Phys. Rev. B.* **97**, 140405 (2018).

## ACKNOWLEDGEMENTS

This work was supported by the W. M. Keck Foundation grant to the Keck Center for Quantum Magnetism at Rutgers University.

## AUTHOR CONTRIBUTIONS

S.W.C. conceived and supervised the project. F.-T.H. conducted magnetic point group analysis. S.W.C. wrote the remaining part.

## COMPETING INTERESTS

The authors declare no competing interests.

## ADDITIONAL INFORMATION

**Correspondence** and requests for materials should be addressed to Sang-Wook Cheong.